CRITICAL EVALUATION OF THE SHEAR-STRESS TRANSPORT (SST) κ−ω TURBULENCE MODEL

Ana Carolina Cellular
Depto. de Engenharia Mecânica, IME – Instituto Militar de Engenharia, 22290-270, Rio de Janeiro – RJ, Brasil
anacellular1@yahoo.com.br

Rafael G. Pestana
Depto. de Engenharia Mecânica, IME – Instituto Militar de Engenharia, 22290-270, Rio de Janeiro – RJ, Brasil
rafael.pestana@terra.com.br

José Carlos C. Amorim
Depto. de Engenharia Mecânica, IME – Instituto Militar de Engenharia, 22290-270, Rio de Janeiro – RJ, Brasil
jcamorim@ime.eb.br

José Diniz M. Abrunhosa
Depto. de Engenharia Mecânica, IME – Instituto Militar de Engenharia, 22290-270, Rio de Janeiro – RJ, Brasil
diniz@ime.eb.br

Abstract. *This paper presents a performance analysis of the shear stress transport κ-ω model in the prediction of a flow over a backward facing step. The commercial code CFX, wich is based on the finite volume method, is used to simulate this flow. The results are compared with predictions made by the standard κ-ε model and by the κ-ω model and with experimental data, verifying the model´s capability of representing the recirculation zones and the pressure recuperation after the backward facing step. It has been concluded that the κ-ω SST model is computationally robust and has a better prediction capability than the traditional models.*

Keywords*: Numerical Simulation, Turbulence Model, Finite Volume, Backward facing step.*

1. Introduction

A great number of turbulent flows of pratical interest have been predicted by two-equation models. Many engineers across the world, motivated by the relative prediction capacity, simplicity and computational robustness, have been employing the $\kappa-\varepsilon$ model to predict turbulent flows of interest, making it the most popular choice among the turbulence models. However, there are various limitations to its use, like its failure in predicting fow separation and its limited capability of predicting flows with fast changing distortions. The excessive eddy viscosity, predicted by the κ-ε in many cases, makes the momentum equations excessively diffusive, supressing fluctuations and separation zones.

The traditional κ-ε model has been widely employed in the central regions of internal flows, while wall functions are adopted in near wall regions. These functions relates the solid surface boundary conditions to the flow outside the viscous sublayer, thus avoiding the direct modelling of the viscous influence and reducing the necessary number of grid points in the near wall region.

Separated flow situations are frequently encountered on engineering applications. Turbulence modelling researches have been actively conducted to make satisfying predictions of these separated flows.

In this context, the backward facing step flow, wich is a separated flow situation widely encountered, is hereby used to analyze the performance of the shear stress transport κ-ω (κ-ω SST) proposed by Menter (1994). The obtained results are compared with the predictions of the traditional κ-ε and κ-ω (Wilcox, 1988) models and with experimental data.

2. Physical Problem

The problem in consideration is an incompressible turbulent flow of a viscous liquid across a channel between infinite plates with area expansion. The average movement is bidimensional and steady.

Two configurations have been simulated. The first one, labeled case A, the channel has a double expansion, while in case B there is only one expansion in the bottom wall. Figure 1 shows schematically the computational domain used in case A simulation, with double expansion. In this configuration, the inlet was placed at a distance equal to ten times the step height (He = 10H) upstream. A channel length of thirty times the step height (30H) was used after the step. It is important to specify a sufficient distance downstream of the reattachment point when adopting a zero diffusion outlet boundary condition to avoid the effects of this condition on the recirculation and recuperation zones (Thangam e Speziale, 1992). The channel height is five times the step height (Hc = 5H) at the inlet and six times the step height (Hc = 6H) at the outlet. The expansion ratio (outlet channel height : inlet channel height) is 1.20, and the Reynolds number is **Re** = $\rho U_c H/\mu$ = 5100, where U_c is the maximum velocity at the inlet and H is the step height. Since the models predictions were compared with results from Le et al. (1997) direct simulation, the physical situation matches those adopted by the mentioned authors.

By contrast, case B predictions were compared with experimental data from Kim et al., 1980, and the utilized physical situation seeks to reproduce the experimental situation adopted by the mentioned authors. The expansion ratio is 1.50 and the Reynolds number is **Re** = $\rho\, U_c\, H/\mu$ = 4.4x10^4, where U_C is the velocity in the center line of the inlet, corresponding to the maximum velocity value in this section, and H_C is the channel height at the outlet (Hc = 3H). The inlet was placed at an upstream distance of five times the step height. Again, the adopted channel lenght after the step is thirty times its height (*30H*) (Thangam e Speziale, 1992).

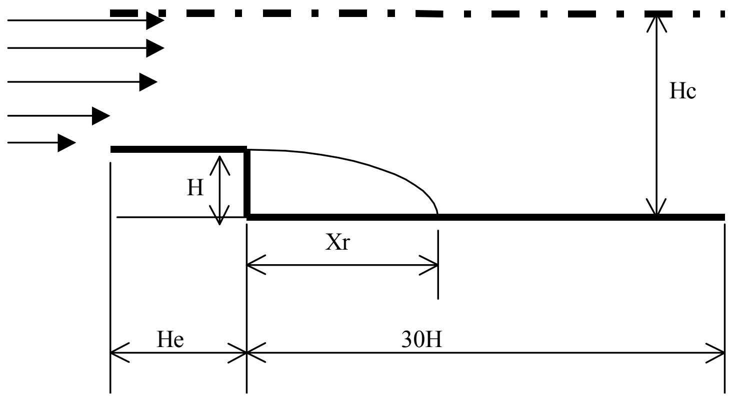

Figure 1 – Computational domain for the channel

3. Governing Equations

The governing equations to represent the mean turbulent, Reynolds averaged and incompressible flow of a viscous fluid are:

$$\frac{\partial \bar{u}_i}{\partial x_i} = 0 \quad , \qquad \frac{\partial}{\partial x_j}\left(\bar{u}_i \bar{u}_j\right) = -\frac{1}{\rho}\frac{\partial \bar{p}}{\partial x_i} + \frac{\partial}{\partial x_j}\left(\upsilon \frac{\partial \bar{u}_i}{\partial x_j}\right) + \frac{\partial \tau_{ij}}{\partial x_j} , \tag{1}$$

where $\bar{u}_i$ are the mean velocity components; $\bar{p}$ is the pressure; υ is the kinematic viscosity; and τ_{ij} is the Reynolds stress tensor ($\tau_{ij} = -\overline{u_i' u_j'}$). Models based on the Boussinesq approximation states that the Reynolds stress tensor depends upon the mean strain-rate tensor S_{ij}, the turbulent kinetic energy κ and the eddy viscosity υ_t :

$$\tau_{ij} = -\frac{2}{3}\kappa\,\delta_{ij} + 2\,\upsilon_t S_{ij} \qquad ; \qquad S_{ij} = \frac{1}{2}\left(\frac{\partial \bar{u}_i}{\partial x_j} + \frac{\partial \bar{u}_j}{\partial x_i}\right) \tag{2}$$

The κ–ω (Wilcox, 1988) and SST κ–ω (Menter, 1994) models establish a relationship between the eddy viscosity υ_t , the dissipation per unit of the turbulence kinetic energy ω and the turbulence kinetic energy κ, as follows:

$$\upsilon_t = (\kappa / \omega)\Psi \tag{3}$$

By the other hand, the κ–ε model for high Reynolds number uses a relationship between the eddy viscosity υ_t , the turbulence kinetic energy κ and its dissipation rate ε, as follows:

$$\upsilon_t = C_\mu \kappa^2 / \varepsilon \tag{4}$$

with C_μ being an empirical constant. The governing equations of the turbulence quantities, modeled for the turbulence kinetic energy (κ), for the dissipation per unit of the turbulence kinetic energy (ω) and for the dissipation rate (ε) can be generally expressed as:

$$\frac{\partial(\bar{u}_j\kappa)}{\partial x_j}=\frac{\partial}{\partial x_j}\left[\left(\upsilon+\frac{\upsilon_t}{\sigma_k}\right)\frac{\partial\kappa}{\partial x_j}\right]+P_\kappa-\Phi \quad ; \qquad P_\kappa=\tau_{ij}S_{ij} \tag{5}$$

$$\frac{\partial(\bar{u}_j\omega)}{\partial x_j}=\frac{\partial}{\partial x_j}\left[\left(\upsilon+\frac{\upsilon_t}{\sigma_\omega}\right)\frac{\partial\omega}{\partial x_j}\right]+\alpha\frac{\omega}{\kappa}P_\kappa-\beta\omega^2+D_\omega \tag{6}$$

$$\frac{\partial(\bar{u}_j\varepsilon)}{\partial x_j}=\frac{\partial}{\partial x_j}\left[\left(\upsilon+\frac{\upsilon_t}{\sigma_\varepsilon}\right)\frac{\partial\varepsilon}{\partial x_j}\right]+C_1\frac{\varepsilon}{\kappa}P_\kappa-C_2\frac{\varepsilon^2}{\kappa} \tag{7}$$

where Φ is the destruction term of the turbulence kinetic energy equation and C_1 , C_2 , C_ω, σ_κ , σ_ε e σ_ω are empirical coefficients of the models. The specification of these parameters and functions is what set apart one model from another. Wilcox´s κ–ω model (1988), referred as WI, Menter´s κ–ω SST model (1994), referred as MT and the traditional high Reynolds κ–ε model, referred as AR, were used in this paper. The models parameters and damping functions are shown in Table 1.

Table 1. Damping functions and constants of the evaluated models

Mod.	**Wilcox (WI)**	**Menter (MT)**	**κ–ε High Re (AR)**
ψ	1.00	$\frac{1.0}{\max[1+\frac{\Omega F_2}{0.31\omega}]}$, where $F_2=\tanh(\phi_2^2)$; $\Omega=\sqrt{\Omega_{ij}\Omega_{ij}}$; $\Omega_{ij}=\frac{1}{2}(\frac{\partial\bar{u}_i}{\partial x_j}-\frac{\partial\bar{u}_j}{\partial x_i})$, $\phi_2=\max(\frac{2\sqrt{\kappa}}{\beta'\omega y},\frac{500\upsilon}{y^2\omega})$	-
β^*	0.09	0.09	-
β	0.075	$0.075F_1+0.0828(1-F_1)$, $F_1=\tanh(\phi_1^4)$; $\phi_1=\min\left\{\max\left(\frac{\sqrt{\kappa}}{\beta'\omega y},\frac{500\upsilon}{y^2\omega}\right),\frac{4\rho\kappa}{CD_{\kappa\omega}\sigma_{\omega,2}\,y^2}\right\}$; $CD_{\kappa\omega}=\max\left(2\rho\frac{1}{\sigma_{\omega 2}\omega}\nabla\kappa\nabla\omega,10^{-10}\right)$	-
σ_κ	2.00	$\frac{1.0}{\left(F_1/\sigma_{k,1}\right)+\left((1-F_1)/\sigma_{k,2}\right)}$	1.00
σ_ω	2.00	$\frac{1.0}{\left(F_1/\sigma_{\omega,1}\right)+\left((1-F_1)/\sigma_{\omega,2}\right)}$	
σ_E	-	-	1.30
α	5/9	5/9	-
D_ω	-	$2(1-F_1)\rho\sigma_{\omega,2}\frac{1}{\omega}\frac{\partial\kappa}{\partial x_j}\frac{\partial\omega}{\partial x_j}$	-
Φ	$\beta^*\omega\kappa$	$\beta^*\omega\kappa$	ε

The non-dimensional constant C_μ is taken as 0.09 in the high Reynolds κ−ε model, while the ε equation constants are taken as C_1=1.44 and C_2=1.92. The κ−ω SST model constants are taken as $\sigma_{k,1}=1.176, \sigma_{k,2}=1.00$, $\sigma_{\omega,1}=2.00$ and $\sigma_{\omega,2}=1.168$.

4. Numerical Method

The CFX code has been used in the numerical simulation. CFX is a multiblock solver for the RANS equations based on a finite volume (Patankar, 1980). The discretization inside the blocks and at block interfaces is done in a conservative and consistent way. Here we are interested in the steady state solution and the solution procedure is based on a time marching concept. The SIMPLEC algorithm for the coupling has been used to correct both the pressure and the velocity fields. The simulations were performed until the normalised maximum residuals of all transport equations were below a value of 10^{-6}. The computational domain is subdivided in two blocks. The first block is before of the step. The second block is attached to first block and extends from the end of the step to the outflow boundary. All grids were refined near the direction normal to the walls and at the beginning of the second block, in the re-attachment point. Thangam e Hur (1991) conducted in this problem a careful grid refinement study based on this finite volume method for grids containing 166x73 to 332x142 mesh points. The conclusion of their study was that a 166x73 mesh yielded results were within acceptable limits. Additional calculations were performed by the same authors that indicate that 200x100 mesh yields a fully grid independent solution. All of the computations conducted in this study were performed using this 200x100 nonuniform mesh.

5. Boundary Conditions

The law of the wall was used at all solid surfaces in its standard two layers shape (Kays e Crawford, 1993). The law of the wall is not formally valid for separated turbulent boundary layers. As the separation point is fixed from the position of the step and the flow field is solved iteratively, the friction velocity u_τ can be processed until convergence is obtained, without introducing great errors with its usage.

In case A, the Reynolds number based on the free shear velocity and step height is **Re** = 5100. The mean axial velocity profile at the inlet ($\bar{u}$ (*y*)) is obtained from the boundary layer profile, for $\mathbf{Re}_\theta$= 670, where θ is the momentum width of the boundary layer. The boundary layer length is δ_{99} = 1,2*H*. In WI and MT models, the free shear condition was adopted as $\kappa = 3.75\text{x}10^{-3}[\bar{u}(y)]^2$ and $\omega = 3.33\partial U/\partial y$, respectively. In the κ–ε model, κ and ε profiles were imposed as $\kappa = 3.75\times10^{-3}[\bar{u}(y)]^2$ and $\varepsilon = 4{,}0\times10^2\,\kappa^2$. In case B, the inlet velocity profile was obtained from the computation of a developed flow in a channel of infinite parallel flat plates. The Reynolds number, based on the free shear velocity and step height, is **Re** = 44.000. At the outlet, a condition of zero diffusion was adopted.

6. Results

Turbulent flow over a backward facing step is a widely used situation as a test case to evaluate turbulence models. Despite its simple geometry, there is separation near the step wall, recirculation followed by reattachment and an adverse pressure gradient. For each simulated situation shall be presented results referred to the reattachment point, mean velocity profiles, Reynolds stresses, friction coefficient and pressure coefficient, which were compared, in case A, to the results of direct simulation by Le et al. (1997) and to experimental data by Kim et al. (1980), in case B.

The position where the shear stress at the wall is zero (τ_w=0) is the reattachment point (X_r/H). Table 2 presents the reattachment points, for the main recirculation, predicted by the models. By analyzing the results, it´s verified that the standard κ−ε model wields the smallest recirculation zone, while the κ−ω and κ−ω SST models predict a recirculation zone larger than the experimental. The secondary recirculation zone, near the step wall, wasn´t correctly predicted by the models, the worst result being the one wielded by the κ−ε model. The κ−ω e κ−ω SST models pratically eliminated this zone in the **Re** = 44000 flow simulation. For **Re** = 5100, these models predicted a secondary recirculation zone with an extension of 0.8H, wich is approximately half of the one obtained by direct simulation (1.76H).

Table 2. Reattachment lengths

	Experimental/DNS	κ−ω	κ−ω SST	κ−ε
Caso A	6.28	7.3	7.0	5.5
Caso B	7.00	7.8	7.5	6.5

Figure 2 presents, in four transversal sections, the mean velocity profiles predicted by the models in case A. In the recirculation zone, the models couldn´t predict the velocity profiles with precision. However, generally speaking, it can be concluded that the profiles predicted by the models have good concordance with the experimental data.

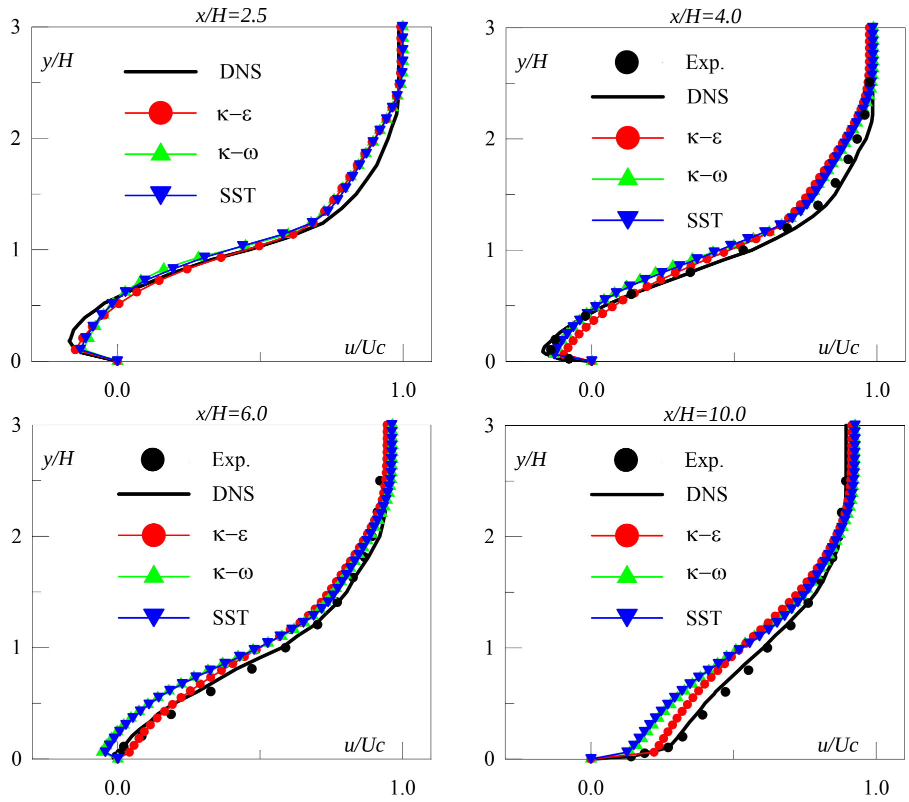

Figure 2: Velocity Profiles for **Re** = 5100

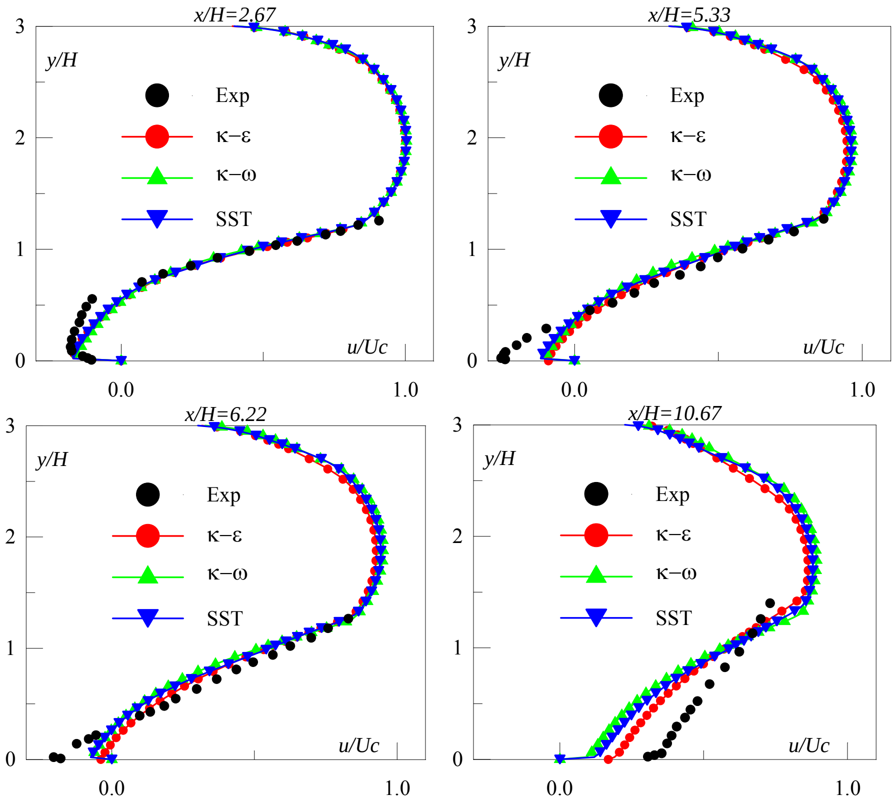

Figure 3: Velocity profiles for **Re** = 44000

Figure 3 presents the mean velocity profiles predicted by the models in case B, also in four transversal sections. In the recirculation zone, again the models couldn´t predict the velocity profiles with precision. In this case, the models also showed a defficient flow recuperation (X_r/H = 10.67).

Turbulent shear stress profiles ($(-\overline{u'v'})/(U_c)^2$) are compared, for case A, in Figure 4, while Figure 5 shows these profiles for case B. From the referred figures, it´s verified that the traditional κ–ε model is the one that predicts the highest values for the turbulent stress, therefore explaining the smallest recirculation zone predicted by the model. Generally speaking, it can be stated that the models had a good performance predicting this parameter.

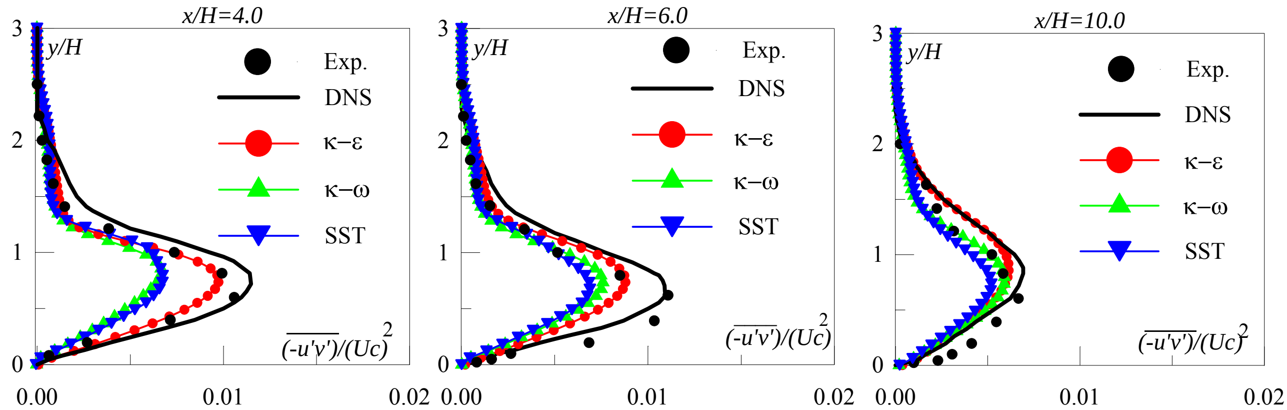

Figure 4: Turbulent shear stress profile ($(-\overline{u'v'})/(U_c)^2$) for **Re** = 5100

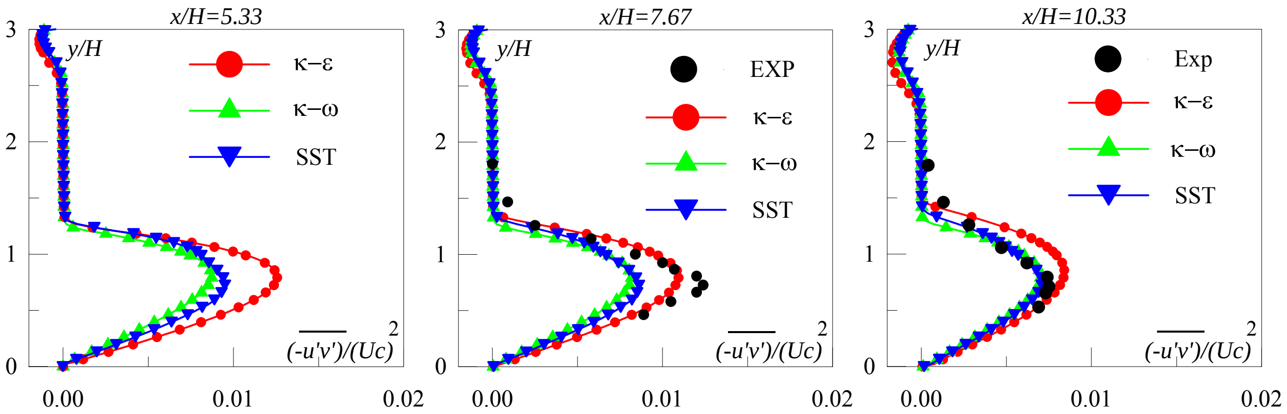

Figure 5: Turbulent shear stress profile ($(-\overline{u'v'})/(U_c)^2$) for **Re** = 44000

Friction coefficient (C_f), defined as $C_f = (2u_\tau^2 / \rho U_c^2)$, where u_τ is the friction velocity and U_c is the highest velocity at the inlet, was evaluated by the law of the wall, in the bottom wall after the step. Figure 6 shows the results obtained by the models. It´s observed from the analysis of this figure that the models couldn´t predict the behavior predicted by the direct simulation, for the case with the smallest Reynolds number. This failure may be caused by the small Reynolds number and the adopted boundary condition. The high Reynolds κ–ε model presents the smallest recuperation rate, but predicts the highest values for the friction coefficient in the final region of the domain.

The pressure coefficient was defined as $C_P = (P-P_c)/(U_c^2)$, where Pc is the pressure over the center line of the inlet, to analyze the pressure distribution. The coefficient variations obtained by the models in the zone after the step are compared, in Figure 7, to the results of the direct simulation by Le et al. (1997), for **Re** = 5100, and to experimental data by Eaton e Johnston (*apud* Thangam e Speziale, 1992), for **Re** = 44000. All models present good predictions on the behavior of the experimental data. The greatest discrepancy related to the experimental data is in the recuperation zone of the flow, where the models have an insufficient pressure recuperation rate and are therefore incapable of predicting the fast variations that occur in this zone.

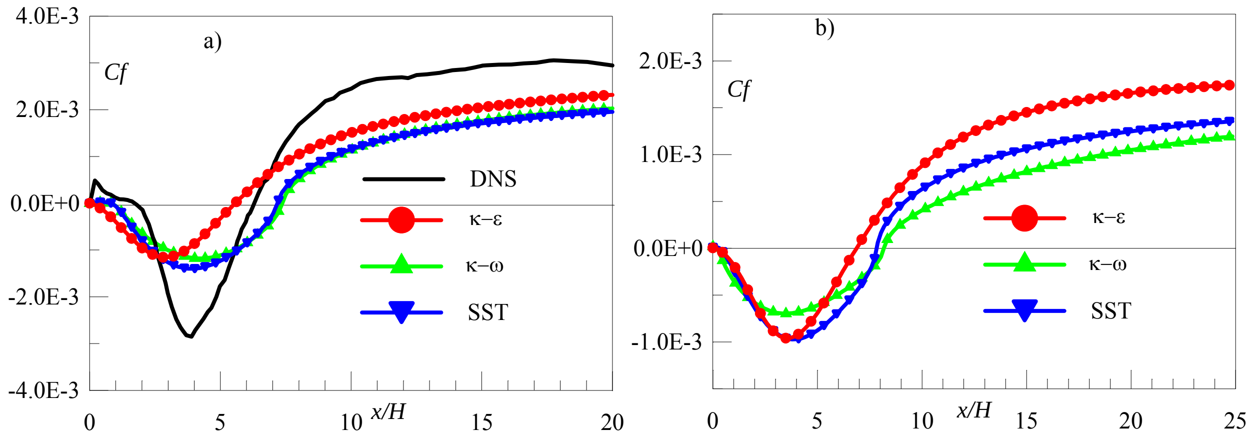

Figure 6: Friction coefficient – a) **Re** = 5100 b) **Re** = 44000

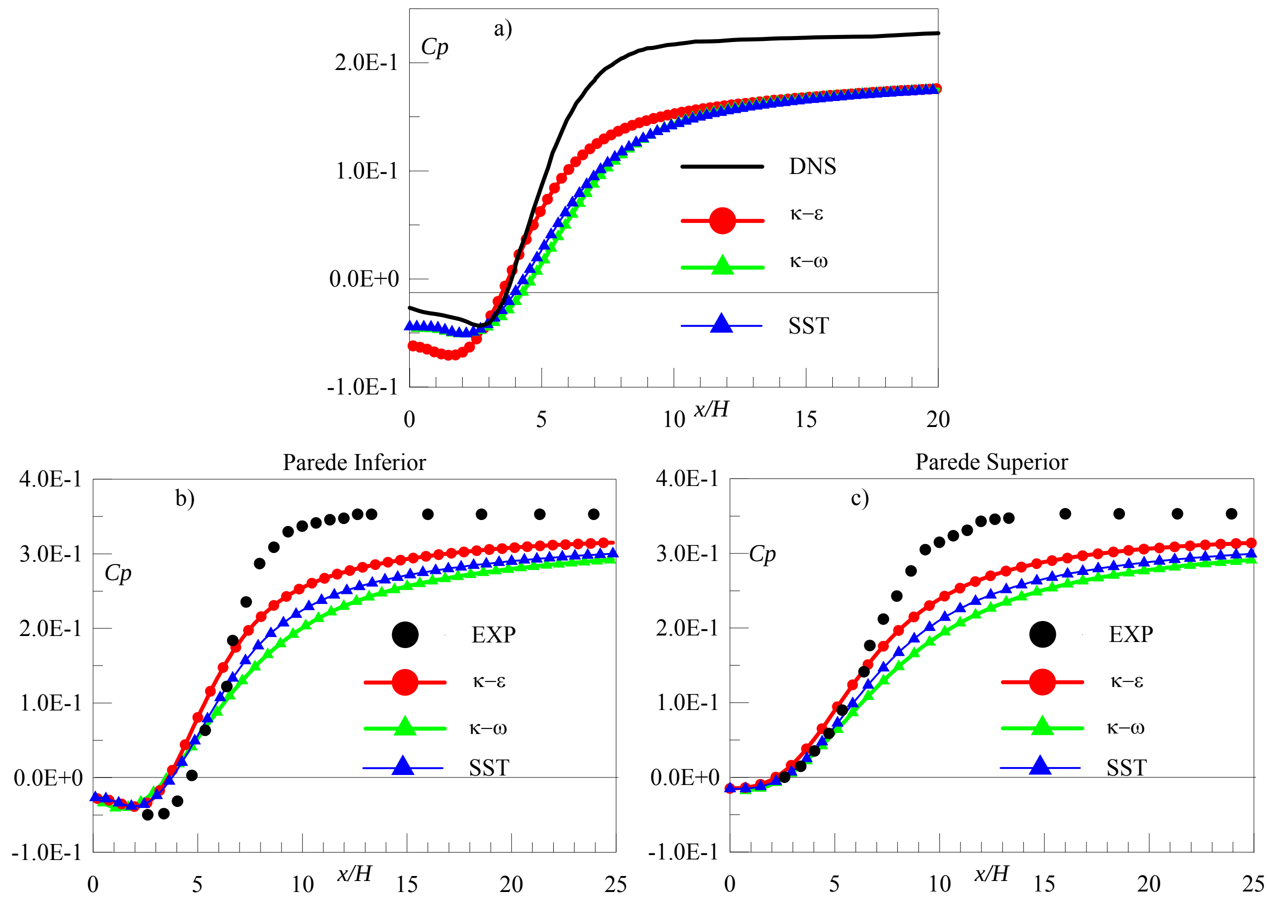

Figure 7: Pressure coefficient – a) **Re** = 5100; b) and c) **Re** = 44000

7. Conclusions

This paper evaluated de two-equation models high Reynolds κ–ε, Wilcox κ–ω (1988) and the κ–ω SST model (Menter, 1994) for a turbulent flow over a backward facing step, with help from direct simulation data (Le et al., 1997).

The κ–ω models showed themselves less diffusive than the κ–ε model. The κ–ω SST model obtained a better behavior than the linear κ–ε model, particularly in its capacity to predict the main and secondary recirculation zones. The κ–ε model understimated the main recirculation zone and effectively eliminated the secondary recirculation zone for both cases, in spite of the high levels of turbulent stress generated by the model. The k-ω SST model was capable to predict reasonably the secondary recirculation zone for the lowest Reynolds number simulation.

However, the κ–ε model made the best prediction of the pressure recuperation, the differences to the other models accentuated for the highest Reynolds number case.

It is worthy of notice that the models didn´t show significant differences in computational terms.

8. References

Kays, W. M., and, Crawford, M. E., 1993, Convective Heat and Mass Transfer, McGraw-Hill;

Kim, J., Kline, S.J., and, Johnston, J. P., 1980, "Investigation of a Reattaching Shear Layer: Flow Over a Backward Facing Step", ASME J. Fluids Eng., Vol. 102, pp. 302-308;

Le, H., Moin, P., and Kim, J., 1997, Direct numerical simulation of turbulent flow over a backward facing step, J. Fluid Mech., vol. 330,pp.349-374;

Menter, F. R., 1994, Two Equation Eddy Viscosity Turbulence Models For Engineering Applications, AIAA J. 32 (8), pp. 1508-1605;

Patankar, S. V., 1980, Numerical Heat Transfer E Fluid Flow, Mcgraw-Hill;

Thangam, S., and Speziale, C. G., 1992, "Turbulent Flow Past a Backward Facing Step: A Critical Evaluation of Two-Eq. Models" , AIAA Journal, Vol. 30, nº 5, pp. 1314-1320;

Thangam, S., and, Hur, N., 1991, "A Highly Resolved Numerical Study of Turbulent Separated Flow Past a Backward Facing Step", International Journal of Engineering Science, Vol. 29, nº 5, pp. 205-211;

Wilcox, D., 1988, Reassessment Of The Scale-Determinig Equation For Advanced Turbulence Models, AIAA J. 26 (11), PP. 1299-1310;

Wilcox, D., 1998, Turbulence Modeling for CFD, DCW Industries Inc.

9. Responsibility notice